Virology 447 (2013) 221–232

Contents lists available at ScienceDirect

Virology

journal homepage: www.elsevier.com/locate/yviro

Capacity of wild-type and chemokine-armed parvovirus H-1PV for inhibiting neo-angiogenesis

Muriel Lavie [a,1], Sofie Struyf [b], Alexandra Stroh-Dege [a], Jean Rommelaere [a], Jo Van Damme [b], Christiane Dinsart [a,*]

[a] Tumor Virology Division, Deutsches Krebsforschungszentrum (DKFZ), Heidelberg, Germany
[b] Laboratory of Molecular Immunology, Rega Institute for Medical Research, K.U. Leuven, Leuven, Belgium

ARTICLE INFO

Article history:
Received 10 July 2013
Returned to author for revisions
30 July 2013
Accepted 20 September 2013
Available online 4 October 2013

Keywords:
Parvovirus
Cancer therapy
Angiogenesis
Kaposi sarcoma
Chemokine

ABSTRACT

Anti-angiogenic therapy has been recognized as a powerful potential strategy for impeding the growth of various tumors. However no major therapeutic effects have been observed to date, mainly because of the emergence of several resistance mechanisms. Among novel strategies to target tumor vasculature, some oncolytic viruses open up new prospects. In this context, we addressed the question whether the rodent parvovirus H-1PV can target endothelial cells. We show that cultures of human normal (HUVEC) and immortalized (KS-IMM) endothelial cells sustain an abortive viral cycle upon infection with H-1PV and are sensitive to H-1PV cytotoxicity. H-1PV significantly inhibits infected KS-IMM tumor growth. This effect may be traced back by the virus ability to both kill proliferating endothelial cells and inhibit VEGF production Recombinant H-1PV vectors can also transduce tumor cells with chemokines endowed with anti-angiogenesis properties, and warrant further validation for the treatment of highly vascularized tumors.

Introduction

In addition to genetic and epigenetic changes that occur during the transformation of a normal cell into a cancer cell, the induction of a tumor vasculature, termed "angiogenic switch" is required to allow tumor propagation and progression (Bergers et al., 2003). Indeed the generation of a tumor blood supply is necessary to provide an adequate amount of oxygen, metabolites, get rid of waste products from the tumor site and trigger metastasis. Induction of the angiogenic switch relies on the tumor-induced change of the local balance between positive (such as VEGF, FGFs) and negative regulators of angiogenesis (Ferrara and Alitalo 1999; Gerwins et al., 2000; Chung et al., 2010). The dependency of tumors on blood supply has led to the development of anti-angiogenic molecules and the design of anti-angiogenic strategies for cancer treatment. Moreover, interference with the tumor blood supply appears as an attractive therapeutic option since it may be effective against a wide range of tumor types. Thus, targeting VEGF pathway with various inhibitors has led to FDA approval of multiple drugs for the treatment of advanced cancer. Such treatment conferred transient clinical benefit, including overall survival (Ferrara, 2010). However, inherent or acquired resistance eventually develops which can lead to more invasive or metastatic potential (Ferrara 2010; Rubenstein et al., 2000; Ebos and Kerbel, 2011). As a consequence, research efforts have focused on search for new anti-angiogenic therapeutic strategies, including oncolytic virus-based therapies (Breitbach et al., 2013).

Some rodent parvoviruses, among them the rat H-1PV, constitute promising candidates for oncolytic virotherapy of cancer. Indeed, they present an intrinsic oncotropism and oncolytic activity as well as an excellent safety profile (Nuesch et al., 2012; Rommelaere et al., 2010). H-1PV belongs to the genus *Parvovirus*. These autonomous parvoviruses are non-enveloped viruses which consist of an icosahedral capsid containing a single-stranded DNA of about 5000 nucleotides (Cotmore and Tattersall, 2007). The parvoviral genome mainly consists of two overlapping transcription units whose expression is under the control of two promoters. The P4 promoter directs the expression of the non-structural proteins (NS1 and NS2) and the P38 promoter drives the expression of the capsid proteins (VP1 and VP2) (Cotmore et al., 2007) and of the non-structural SAT protein (Zadori et al., 2005). NS1 protein is a mainly nuclear, phosphorylated, multifunctional protein of about 83 kDa that is required for the replication of the viral genome, transactivation of the P38 promoter and is the main effector of parvoviral cytotoxicity (Li and Rhode, 1990; Caillet-

* Correspondence to: Tumor Virology Division, F010, Deutsches Krebsforschungszentrrum, Im Neuhenheimer Feld 242, D-69120 Heidelberg, Germany. Fax: +49 6221 424962.
E-mail address: c.dinsart@dkfz.de (C. Dinsart).
[1] Present address: Center for Infection and Immunity of Lille, INSERM U1019, CNRS UMR8204, Institut Pasteur Lille, Université de Lille Nord, France.

0042-6822/$ - see front matter © 2013 Elsevier Inc. All rights reserved.
http://dx.doi.org/10.1016/j.virol.2013.09.019

Fauquet et al., 1990; Nuesch et al., 2008). The oncoselectivity of PVs is usually not due to a better virus uptake by transformed cells but to more efficient PV replication in these cells. In particular, conversion of the viral single-stranded DNA genome into double-stranded replication forms and transcription of these duplex forms depends on factors that are deregulated during oncogenic transformation (Cornelis et al., 1988). Moreover, the lack of preexisting antiviral immunity in most humans plays in favor of the efficacy of PV use in cancer treatment. Numerous data have been accumulated, showing the tumor suppressive activity of parvoviruses against various models of rodent and human cancers. PVs can be either used in their natural form (Geletneky et al., 2010; Angelova et al., 2009; Rommelaere et al., 2010) or armed to deliver toxic or immunostimulatory transgenes (Enderlin et al., 2009; Wetzel et al., 2007; Dempe et al., 2012; Haag et al., 2000; Giese et al., 2002). Based on the promising *in vitro* and preclinical evidence of anti-tumor properties, the rat parvovirus H-1PV is currently used in a phase I/IIa clinical trial for treatment of patients with glioblastoma multiforme (Geletneky et al., 2012). In addition to its oncolytic activity, immunostimulating effects are likely to participate in the suppression of tumors by PVs (McKisic et al., 1998; Moehler et al., 2003, 2005; Sieben et al., 2012; Grekova et al., 2012; Bhat et al., 2011).

The pathogenicity of rodent parvoviruses is restricted to proliferating tissues and decreases from the fetus to the adult for which the infection remains asymptomatic (Rommelaere and Cornelis, 1991). Pathogenic features in persistently infected hosts indicate that some rodent parvoviruses display a tropism for endothelial and vascular smooth muscle cells (Siegl, 1984; Ball-Goodrich et al., 1998; Jacoby et al., 1996; Cole et al., 1970; Margolis and Kilham, 1970; Jacoby et al., 2000). This endotheliotropism raises the possibility that, in addition to a direct anti-tumor activity, parvoviruses may also target and exert toxicity on tumor vasculature, provided that the vessels are actively growing (neo-angiogenesis). The present study aimed to evaluate the anti-angiogenic potential of (i) H-1PV on Kaposi sarcoma (KS-IMM) cells, a human model for vascular tumors (Albini et al., 1997; Mesri et al., 2010) and (ii) H-1PV-based recombinant viruses armed to deliver two potent anti-angiogenic chemokines: IP-10/CXCL10 and PF-4var/CXCL4L1.

The interferon gamma inducible protein-10 (IP-10) and platelet factor-4 variant (PF-4var) belong to the CXC chemokine subfamily that lack the sequence Glu-Leu-Arg (ELR motif) at their NH_2-terminus (ELR-negative chemokines). Most chemokines of this subfamily constitute potent inhibitors of angiogenesis (Strieter et al., 1995; Keeley et al., 2010). Thus, IP-10 has been shown to suppress endothelial cell differentiation, migration and proliferation (Loetscher et al., 1996). Moreover it recruits activated T-cells and NK cells via binding to the G protein-coupled CXCR3 receptor (Loetscher et al., 1996; Taub et al., 1993). Anti-tumor effects of IP-10 are still controversial. IP-10 and its receptor have been reported to have dual actions on tumorigenesis, depending on the model and method of delivery (Zipin-Roitman et al., 2007; Liu et al., 2010, 2011; Narvaiza et al., 2000; Giese et al., 2002; Enderlin et al., 2009; Dempe et al., 2012). Although the mechanism of IP-10-mediated tumor suppression is not fully elucidated, both its anti-angiogenic activity and immunomodulatory properties are required (Angiolillo et al., 1995; Farber, 1997).

Platelet Factor-4 (CXCL4/PF-4) was the first chemokine shown to inhibit angiogenesis. CXCL4L1/PF-4var was isolated from thrombin-stimulated platelets and differs from PF-4 in three carboxy-terminal amino acids (Green et al., 1989; Eisman et al., 1990; Struyf et al., 2004). PF-4var was found to be a more potent angiostatic and anti-tumoral chemokine compared to PF-4 in various *in vitro* and *in vivo* assays (Vandercappellen et al., 2011; Struyf et al., 2007). Moreover PF-4var presents chemoattractive activity towards activated T-cells, human NK cells and human immature dendritic cells (Struyf et al., 2011). Both CXCR3 receptor and glycosaminoglycans are involved in the activities of PF-4var (Struyf et al., 2011). PF-4var antitumoral activity was predominantly mediated through inhibition of angiogenesis and induction of apoptosis (Vandercappellen et al., 2011).

In this manuscript, we show that proliferating normal HUVEC and immortalized Kaposi sarcoma-derived, KS-IMM human endothelial cells are sensitive to H-1PV toxicity *in vitro*. However, relatively high virus doses have to be used, due to the fact that the cells undergo an abortive infection which does not lead to progeny virus production and spread. Interestingly, H-1PV infection of highly angiogenic KS-IMM cells significantly reduces their tumor-forming ability after s.c. implantation into recipient mice, thus demonstrating the potential of H-1PV for treatment of vascular tumors. Notably, infection with H-1PV-based vectors inhibits the expression of the key angiogenesis factor, VEGF, in endothelial cells, irrespective of their arming with chemokine transgenes. Finally, we show that active anti-angiogenic chemokines are produced upon transduction of KS-IMM cells with H-1PV-based recombinant vectors. Altogether these data warrant further validation of chemokine-delivering H-1PV for tumor neo-angiogenesis suppression.

Results

Primary and immortalized endothelial cells are sensitive to H-1PV cytotoxicity in vitro

To determine the capacity of H-1PV to infect human endothelial cells, normal primary (HUVEC) and immortalized (KS-IMM) endothelial cells were infected with H-1PV at increasing multiplicities of infection (MOI). The viability of the endothelial cells was determined by MTT assay at day 1, 2, and 3 post-infection (p.i.), and compared to the survival of the highly H-1PV-permissive human embryonic kidney NB-324K cells (Fig. 1a–c). Both HUVEC and KS-IMM cells were found to be sensitive to H-1PV infection in a dose-dependent manner, yet to various degrees. Indeed, at the highest MOI tested (30 RU/cell), the viability of KS-IMM cells dropped to less than 5%, whereas the survival HUVEC cells was around 20% at day 3 p.i. In contrast, the viability of H-1PV-infected HUVEC cells was reproducibly lower than that of KS-IMM cells at lower MOIs. Compared with HUVEC and KS-IMM cells, control NB-324K cells showed a greater drop in survival over post-infection time, with close to 95% of dead cells at day 3 following infection at a multiplicity as low as 0.3 RU/cell (Fig. 1c). This high sensitivity of NB-324K cells can be ascribed to their full permissiveness for H-1PV production and propagation (Dempe et al., 2012). At day 3 post-infection, cell lysis was evaluated by the release of lactate dehydrogenase (LDH) in the cell culture medium (Fig. 1d). The levels of LDH in the cell culture medium increased with the virus dose tested: up to 50% (HUVEC cells) and 80% (KS-IMM and NB-324K cells) of total LDH, after infection at a MOI of 30 RU/cell. This indicates that the decrease in cell viability is likely due to the induction of cell lysis upon H-1PV infection rather than a cytostatic effect on the cell growth.

H-1PV infection leads to an abortive viral cycle in endothelial cells

The susceptibility of HUVEC and KS-IMM cells to H-1PV infection prompted us to investigate whether these cells were able to propagate the virus. To this end, cells were infected at a MOI of 0.5 PFU/cell and the production of progeny viruses was monitored over 6 days p.i. As shown on Fig. 2a, whereas NB-324K cells sustained a 2000-fold amplification of the virus inoculum at day 2 p.i., KS-IMM and HUVEC cells produced only marginal levels of progeny viruses (about 10-fold increase compared to the virus

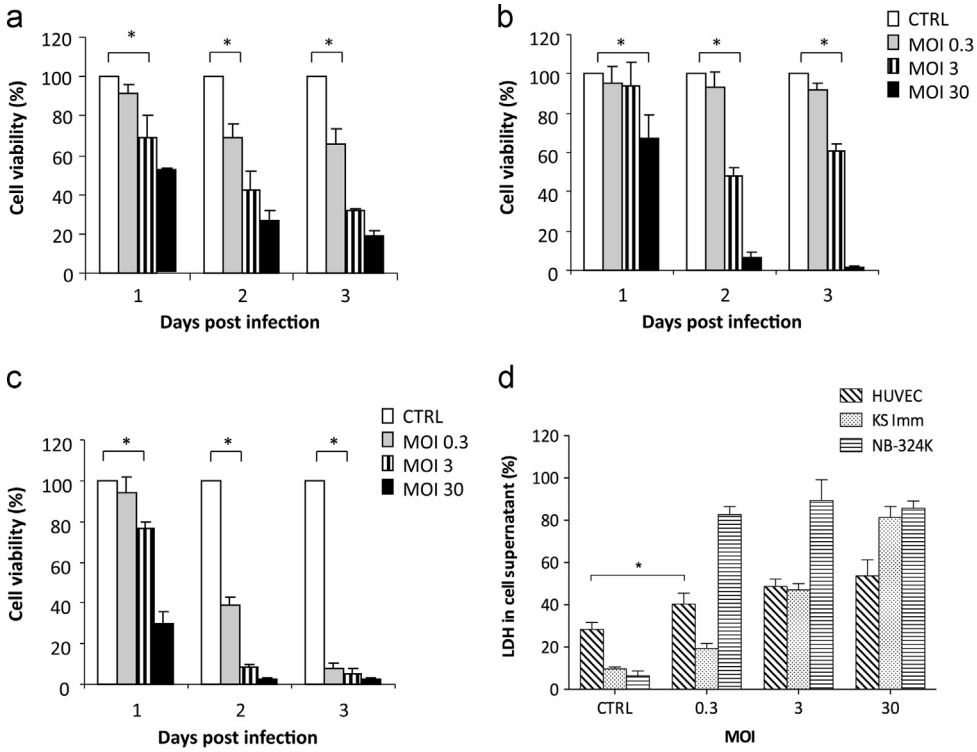

Fig. 1. Cytotoxic effects exerted by H-1PV on normal endothelial (HUVEC) and immortalized Kaposi sarcoma (KS-IMM) cells. HUVEC (a), KS-IMM (b) and control virus-producer NB-324K (c) cells were infected with wild-type (wt) H-1PV at different multiplicities of infection (MOI): mock (buffer)-treated (CTRL), 0.3, 3 and 30 RU/cell. The cell viability of virus-infected and mock-treated cells was determined by MTT assay at days 1–3 post-infection. Values are expressed relative to mock-treated controls virus lytic activity was measured through quantification of the cytoplasmic release of LDH into the culture medium at day 3 post-infection. Values are expressed as a percentage of total LDH present in the infected or mock-treated (CTRL) cultures (d). Means $\pm$SD from three independent experiments carried out in triplicate. *$p < 0.05$ in Wilcoxon signed rank test (cell viability) or Mann–Whitney test (cell lysis). (a) HUVEC, (B) KS Imm, (c) NB-324K and (d) Cell lysis.

inoculum). This indicates that these human endothelial cells, though susceptible to H-1PV infection and toxicity, are poorly competent with respect to their ability to produce progeny viruses. In order to identify which step(s) of the viral cycle is impaired in KS-IMM and HUVEC cells, the expression of the viral proteins was analysed by Western blotting. As seen in Fig. 2b, high levels of NS1 accumulated in both KS IMM and HUVEC cells in infected cells from day 1 to 3 post-infection, (MOI=3 RU/cell), and decreased at later times. A similar NS1 production was sustained by NB-324K cells but dropped at an earlier time between day 2 and day 3 p.i. NS1 is considered as the major mediator of parvovirus-induced cytotoxicity (Caillet-Fauquet et al., 1990; Momoeda et al., 1994; Brandenburger et al., 1990; Li and Rhode, 1990). The expression of this protein in endothelial cells is thus consistent with the observed killing effect of the virus on these cells (Fig. 1a–d), while the faster fading of the NS1 signal in NB-324K vs endothelial cells can be traced back to the above-mentioned killing of the former cells for an extended time (Fig. 1c). The accumulation of the small NS2p protein was slightly, yet reproducibly, lower in HUVEC cells compared with the two other cells. Striking differences in the accumulation of the capsid (VP1 and VP2) proteins were observed between endothelial and NB-324K cells. High steady-state levels of capsid proteins were detected in NB-324K cells throughout the time period studied, in agreement with the production of progeny virions in these cells. In contrast, KS-IMM and HUVEC cells failed to accumulate VP proteins over time p.i., suggesting that the synthesis and/or stability of VPs was impaired in these cells. Since only trace amounts of NS1 are sufficient to efficiently transactivate the viral P38 promoter programming the capsid-encoding genes (Lorson et al., 1996), we hypothesize that a post-transcriptional event is likely to be responsible for the low steady-state levels of VPs in endothelial cells, in particular VP instability. In support of this, it has been reported that in murine cells, the reduction in VP accumulation is not due to reduced viral protein synthesis but rather to impaired capsid assembly, which render capsid proteins unstable and, hence, susceptible to degradation (Cotmore et al., 1997). In order to determine whether earlier steps of the parvoviral cycle are impaired in endothelial cells, we investigated viral DNA replication in infected KS-IMM and HUVEC cells. For this purpose, viral DNA was extracted at two time points post-infection (18 and 42 h) and analysed by Southern blotting using a NS1-specific DNA probe. As shown in Fig. 2c, NB-324K cells sustained the time-dependent accumulation of both monomeric (mRF) and dimeric (dRF) DNA replicative forms, as well as the packaging-coupled displacement of single-stranded (ss) genomes. In contrast, only mRF forms could be detected in KS-IMM and HUVEC cells, which sustained very limited DNA amplification. Altogether, these data indicate that the abortive nature of endothelial cell infection with parvoviruses can be traced back to the impairment of several steps of the viral life-cycle, limiting the accumulation of both DNA replication intermediates and capsid proteins.

H-1PV infection inhibits the growth of KS-IMM tumors in vivo

Although KS-IMM and HUVEC cells are not fully permissive to H-1PV infection, *i.e.* fail to produce and propagate the virus, our results show that these cells are sensitive to H-1PV toxicity when high enough doses of virus are used. This sensitivity indicates that some endothelial cells may constitute targets for parvovirus infection and toxicity, provided that they are proliferating, and suggests that the endotheliotropism of H-1PV might contribute to the tumor-suppressive activity of this virus through the inhibition of tumor neo-angiogenesis. This prompted us to investigate the anti-tumor potential of H-1PV against KS-IMM xenografts. To this end, 3×10^6

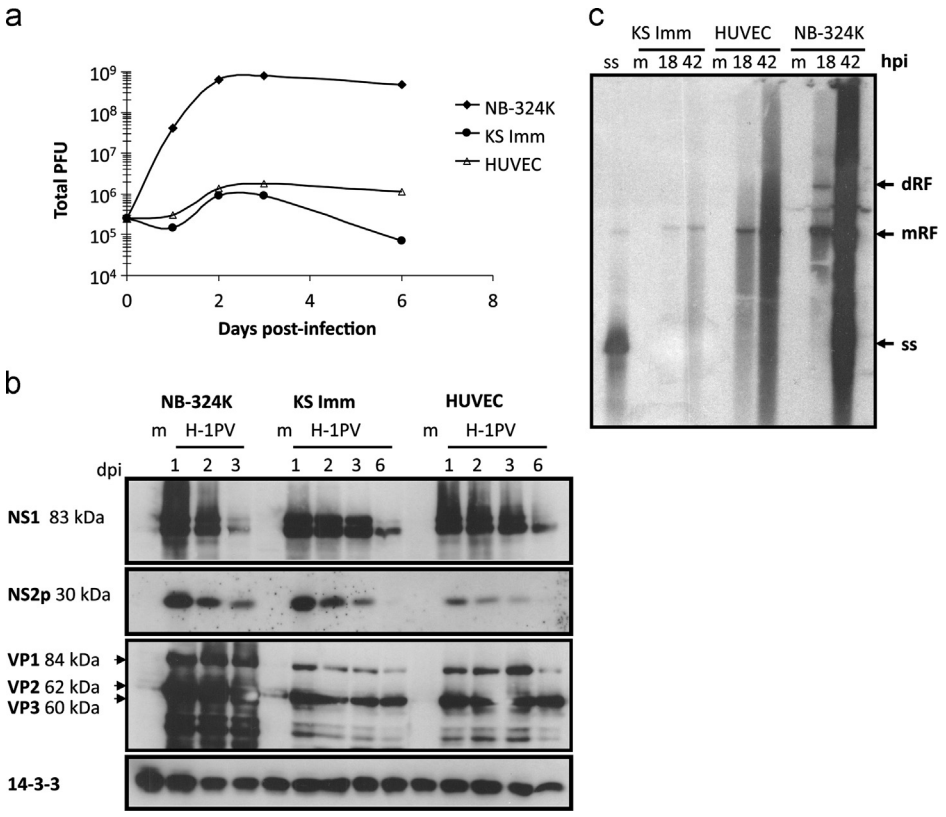

Fig. 2. Abortive infection of endothelial cells by H-1PV. (a) Production of progeny virus after infection of endothelial cells. 5×10^5 KS-IMM, HUVEC and NB-324K cells were infected with H-1PV (MOI of 0.5 PFU/cell). The amounts of infectious particles (intra- and extracellular; total PFU) recovered at the indicated times post-infection were determined by plaque assays. (b) Viral non-structural (NS1, NS2) and capsid (VP1, VP2/VP3) protein accumulation in H-1PV-infected endothelial cells. KS-IMM, HUVEC and control NB-324K cells were mock-treated (m) or infected with H-1PV (MOI of 3 RU/cell) and incubated for the indicated days post-infection (dpi). Cell extracts were then processed for Western blotting using primary antibodies specific for NS1, NS2p and VP proteins and horseradish peroxidase-conjugated secondary antibodies. 14-3-3 proteins were used as the loading control. (c) Viral DNA replication in H-1PV-infected endothelial cells. Cells were infected with H-1PV at a MOI of 3 PFU/cell. At 18 h and 42 h post infection, viral DNA replicative forms purified from cell lysates were separated by agarose gel electrophoresis and subjected to Southern blotting. Viral replicative intermediates were revealed using a NS1-specific ^{32}-P labelled DNA probe. m: mock-treated, mRF: monomeric replicative form, dRF: dimeric replicative form. ss: single stranded viral DNA was used as size marker.

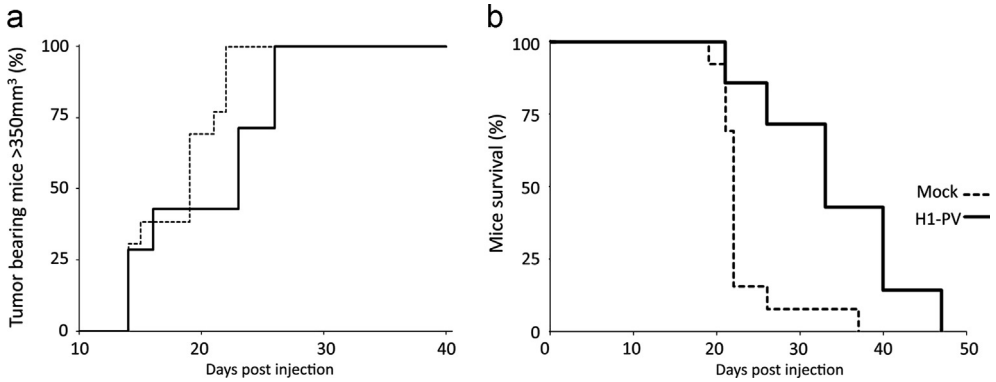

Fig. 3. H-1PV-induced inhibition of human KS-like tumor development. 3×10^6 KS-IMM cells were mock (buffer)-treated or infected with H-1PV at a MOI of 12 RU/cell. The cells were mixed with Matrigel and subcutaneously implanted into the right flank of Balb/c nude mice ($n=13$: mock-treated, $n=7$: H-1PV-infected). Tumor development was monitored over time. The percentage of mice bearing a tumor larger than 350 mm^3 (a) and mouse survival (b) are plotted as a function of time post-implantation. The results represent one experiment out of two.

KS-IMM cells were infected with H-1PV (MOI of 12 RU/cell) and subcutaneously implanted into nude Balb/c recipient mice. A control group was inoculated with mock (buffer)-treated cells. Tumors became palpable in controls 12–14 days after cell inoculation, and tumor volumes were measured three times a week over a 55-day period. As shown on Fig. 3a, all the mice developed fast growing tumors, irrespective of whether they were H-1PV-treated or not. However a significant delay in tumor development was observed in the group of animals that received H-1PV-infected KS-IMM cells compared with the group receiving mock-treated cells. This was most apparent the lower percentage of mice bearing tumors larger than 350 mm^3 at day 20 post inoculation in the group of animals that were engrafted with virus-treated cells, compared with the control group (Fig. 3a). As a consequence, a significant increase in the survival time of the animals belonging to the H-1PV-treated group was observed (Fig. 3b). Altogether, our results show that H-1PV can target and inhibit the growth of endothelial tumors. However this effect is transient, and high doses of H-1PV are required to inhibit the

growth of KS Imm tumor cells *in vitro* and *in vivo*. We have previously shown that the oncosuppressive capacity of H-1PV in different tumor models could be enhanced by arming this parvovirus with immunostimulatory transgenes (Haag et al., 2000; Dempe et al., 2012). This led us to investigate the anti-angiogenic potential of parvovirus H-1PV vectors armed with angiostatic chemokines, hypothesizing that expression of these molecules might improve the efficacy of H-1PV in the treatment of highly vascularized tumors such as KS-IMM tumors.

The kinetics and levels of H-1PV-mediated transduction of angiostatic PF-4var/CXCL4L1 and IP-10/CXCL10 in endothelial cells are cell-type and chemokine-dependent

Recombinant vectors (Chi-H1, Dempe et al., 2012) armed with angiostatic chemokines IP-10/CXCL10 or PF-4var/CXCL4L1 (Chi-H1/IP-10 and Chi-H1/PF-4var, respectively) were produced and examined for their transduction capacity. In a first step, KS-IMM and HUVEC cells were infected with the recombinant viruses at a MOI of 3 RU/cell, and chemokines secreted in the culture media were measured at various days post-infection using specific ELISAs. Infected KS-IMM cells secreted IP-10 and PF-4var with a peak of daily production at day 2 p.i, while the highest chemokine production took place earlier (day 1 p.i.) in HUVEC cells (Fig. 4). In both cell types accumulated levels of the chemokines reached a plateau from day 3 p.i. on. Similar maximal cumulative levels of PF-4v (40–50 ng/ml) were measured in the supernatants from both KS-IMM and HUVEC cells. Surprisingly cumulative IP-10 concentrations were reproducibly ($n=3$) 5-fold higher in the supernatants of transduced KS-IMM cell cultures (300 ng/ml) compared with those of HUVEC cultures (60 ng/ml). Moreover the accumulated levels of IP-10 on day 3 p.i. exceeded the sum of daily productions on days 1–3. Since no IP-10 induction was observed after infection of KS-IMM cells with the control (empty) vector, above-accumulation IP-10 values are most likely due to an autocrine stimulation of IP-10 production in Chi-H1/IP-10-infected KS-IMM cells. The concentrations of PF-4var and IP-10 in KS-IMM supernatants are in the range needed for their activity *in vitro* (Struyf et al., 2011; Bodnar et al., 2006).

Virus-transduced IP-10 and PF-4var inhibit KS-IMM endothelial cell proliferation and angiogenesis in vitro

We next analysed the biological activity of the chemokines produced upon transduction of KS-IMM cells. The supernatants of KS-IMM cultures infected with Chi-H1/IP-10 or Chi-H1/PF-4var vectors (MOI=3 or 12 RU/cell) were harvested at day 3 post-infection, and chemokine concentrations were determined by ELISA (Fig. 5a). A 2-fold increase in chemokine concentrations was observed when a 4-fold higher dose of virus was applied to the cells. The chemokine levels in the supernatants of empty vector (Chi-H1/Δ800) or non-infected cells were below the detection limit (≤ 2 ng/ml). Conditioned medium (CM) was harvested from infected cell cultures (Fig. 5a). Untreated (naïve) KS-IMM cells were then incubated for 72 h in the presence of CM and cell viability was assessed by MTT assays (Fig. 5b). No significant difference in cell viability was observed when KS-IMM cells were incubated with CM from cells infected with Chi-H1/Δ800, Chi-H1/IP-10 or Chi-H1/PF-4var at a MOI of 3 RU/cell (Fig. 5b, left part). Only a slight decrease in the number of viable cells (90% of the mock-treated control) was detected after incubation with CM from cells infected with Chi-H1/Δ800 at a MOI of 12 RU/cell. In contrast, the number of viable cells dropped after incubation with CM from cells infected at this MOI with Chi-H1/IP10 (50%) and Chi-H1/PF-4var (70%) (Fig. 5b, right part). This loss of viable cells was unlikely to result from cell destruction, since the lytic activity of both chemokine-armed vectors was similar to that of Chi-H1/Δ800 in infected donor KS-IMM cultures, as measured by LDH assays (data not shown). This suggests that the decrease in viable cell numbers in KS-IMM cultures exposed to chemokine-containing CM (Fig. 5b) is due to an inhibitory effect of virally-transduced IP-10 and PF-4var on the proliferation of endothelial cells, rather than their integrity. This conclusion is in agreement with the known properties of these angiostatic chemokines on the proliferation of endothelial cells *in vitro* (Strieter et al., 2005; Dubrac et al., 2010). Since IP-10 and PF-4var are known to signal via the G protein-coupled receptor CXCR3 (Struyf et al., 2011), we analysed the expression of CXCR3 in KS-IMM cells by RT-PCR, using total RNA extracts from mock-treated and virus-infected cells.

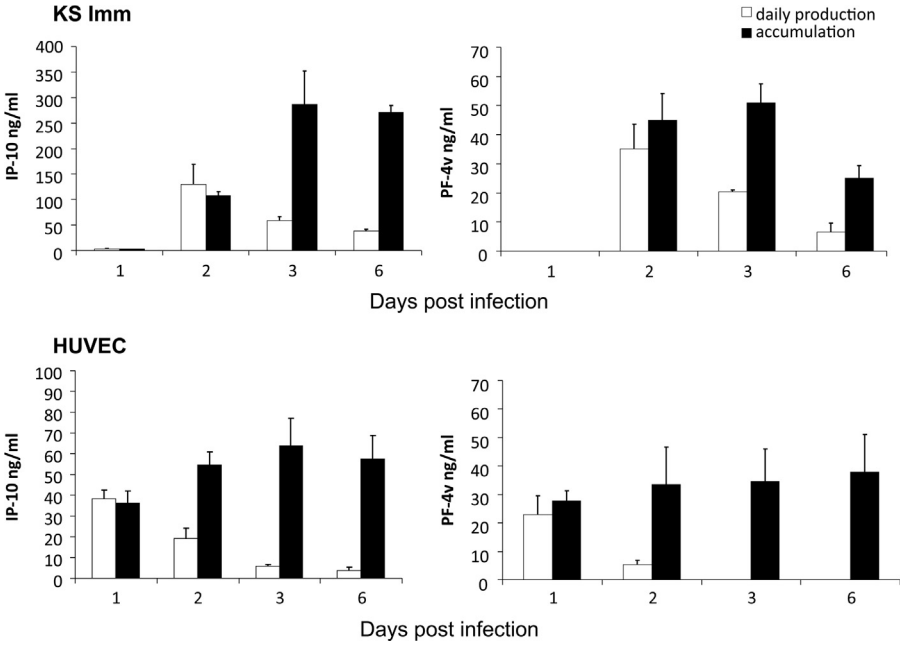

Fig. 4. Daily and cumulative secretion of the chemokines PF-4var and IP-10 after transduction of endothelial cells with recombinant H-1PV-based vectors. 5×10^5 KS-IMM and HUVEC cells were infected with IP-10 or PF-4var-transducing Chi-H1/based vectors at a MOI of 3 RU/cell. Cell supernatants were analysed at indicated days post-infection for their chemokine concentrations using specific ELISAs. Values are means ± SD of three measurements from a representative infection (out of three).

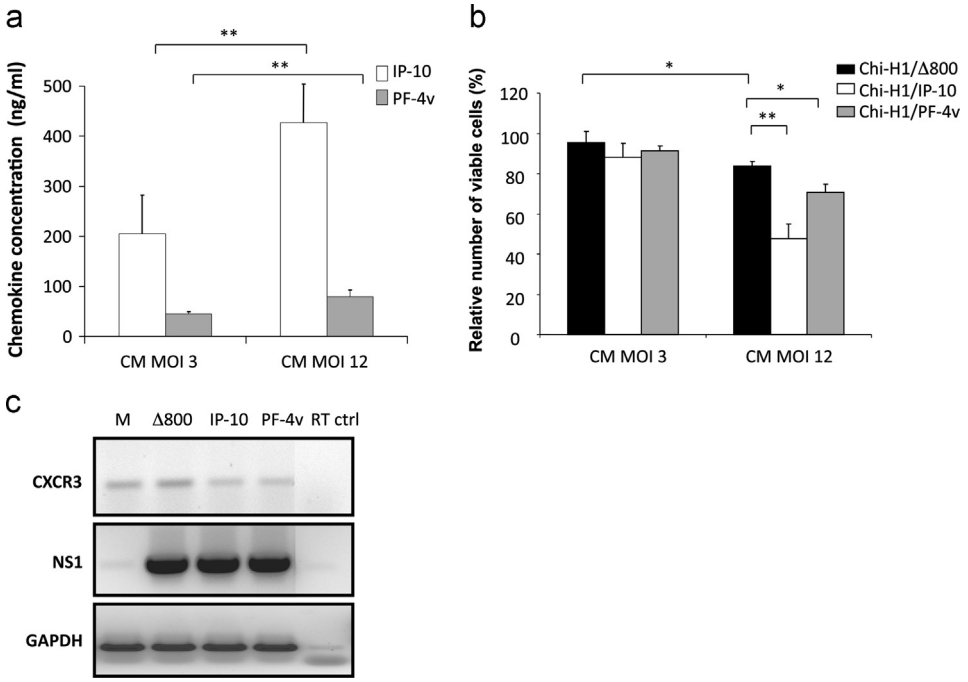

Fig. 5. Anti-proliferative effects of the conditioned media from Chi-H1/IP-10 and Chi-H1/PF-4var-infected KS-IMM cells. (a) Recombinant vector dose-dependency of the chemokine levels secreted by KS IMM cells. 4.5×10^4 KS IMM cells were infected with Chi-H1/IP-10 or Chi-H1/PF-4var at MOI of 3 and 12 RU/cell. At day 3 post-infection, the supernatants were harvested and the levels of IP-10 and PF-4var determined by specific ELISAs. Values represent means ± SD from three independent experiments carried out in triplicate. $^{**}p < 0{,}01$, $^{*}p < 0{,}05$ in the Mann–Whitney test. (b) Viability of KS-IMM cells incubated with chemokine-transduced conditioned media (CM). KS-IMM cells were infected with Chi-H1/Δ800, Chi-H1/IP-10 or Chi-H1/PF-4var at a MOI of 3 and 12 RU/cell or mock-treated. At day 3 post-infection, the cell supernatants (CM) were harvested and transferred to untreated KS-IMM cells. After 72 h incubation, the cell viability was determined by MTT assay. The values are expressed as percentages of the value obtained for mock-treated cultures. Values are means ± SD from three independent experiments each carried out in triplicate. $^{**}p = 0{,}001$, $^{*}p = 0{,}005$ in the Mann–Whitney test. (c) Expression of CXCR3 receptor in KS-IMM cells. 5×10^5 KS-IMM cells were mock-treated (M) or infected with the viral vectors: Chi-H1/Δ800, Chi-H1/IP-10 or Chi-H1/PF-4var (MOI of 3 RU/cell). At day 3 post-infection, total RNA was extracted from the cells and reverse-transcribed. cDNAs were amplified by PCR using primers specific for CXCR3-, viral NS1- or GAPDH-transcripts, and visualized on 1% ethidium bromide-stained agarose gels. RTctrl: control reactions in the absence of reverse transcriptase.

The levels of viral (NS) and cellular (GAPDH) transcripts were also determined as internal controls for virus infection and total RNA matching, respectively. As shown on Fig. 5c, a specific amplification product corresponding to CXCR3 mRNA was obtained from mock and infected cells. The specificity of the reaction was confirmed by the presence of NS transcripts in vector-infected but not mock-treated cells (Fig. 5c). No amplification product was obtained when reverse transcriptase was omitted from the reaction (Fig. 5c, RTctrl) indicating the absence of contaminating genomic DNA. The steady-state level of CXCR3 transcripts was not modified by vector infection.

We next investigated the anti-angiogenic potential of the transduced chemokines using an *in vitro* assay. Untreated KS-IMM cells were seeded on matrigel-coated dishes and incubated with the CM collected from donor KS-IMM cultures infected (MOI = 12 RU/cell) with the different parvoviral vectors, as described for Fig. 5. The results were normalized to CM from KS-IMM cells infected with the empty vector, in order to take the toxic effects of the vector into account. KS-IMM cells formed a network of tube-like structures within 12–18 h (Fig. 6a). A significant inhibition of tube formation was observed when the cells were incubated with CM containing IP-10 or PF-4var, as compared to the control CM (Fig. 6a). Although the concentration of PF-4var was about 4-times lower than that of IP-10 (90 ng/ml and 400 ng/ml, respectively), the inhibitory effects of PF-4var-containing CM on network formation were stronger in comparison with IP-10 (40% versus 20% inhibition, Fig. 6b). These results are consistent with previous reports showing that, under *in vitro* conditions, PF-4var inhibits angiogenesis at lower concentrations than IP-10 (Struyf et al., 2007; Vandercappellen et al., 2011; Bodnar et al., 2006). As mentioned above, incubation of KS-IMM cultures with chemokine-containing CM for 3 days resulted in a reduction of the number of viable cells compared with control (empty vector treatment) CM (Fig. 5b). In order to determine whether the inhibitory effects of chemokine-containing CMs on *in vitro* angiogenesis was due to reduced growth of the viable cell population, the size of this population was determined by MTT assay after the 12–18 h incubation used in the angiogenesis assay. No significant difference in the relative number of viable cells was observed between cultures exposed for this short period of time to CM from vector, compared with mock-treated cells (Fig. 6c). Taken together, our data show that the CMs of Chi-H1/PF-4var and Chi-H1/IP-10-infected KS-IMM cells contain biologically active chemokines which exert both a rapid suppression of the angiogenic phenotype of endothelial cells and an inhibition of the proliferation of these cells later on.

Infection with parvoviral vectors reduces the expression of VEGF-A in KS-IMM cells

Kaposi's sarcoma cells are known to produce VEGF-A which constitutes a key angiogenic stimulator and a critical mitogen in the development of the tumor (Masood et al., 1997; Sodhi et al., 2000). Hence, this growth factor is a good candidate target for anti-angiogenesis-based tumor therapy (Ellis and Hicklin, 2008). This prompted us to test whether chemokine-armed parvoviral vectors may modify the expression of VEGF-A in KS-IMM cells, besides exerting above-mentioned toxic, cytostatic and anti-angiogenic effects. To this end, KS-IMM cells were infected at different MOIs with empty and recombinant parvoviral vectors, and total RNA was extracted at day 2 post-infection. After reverse-transcription, VEGF-A cDNAs were quantified by real time PCR, and their abundance in vector-treated cells was expressed relative to

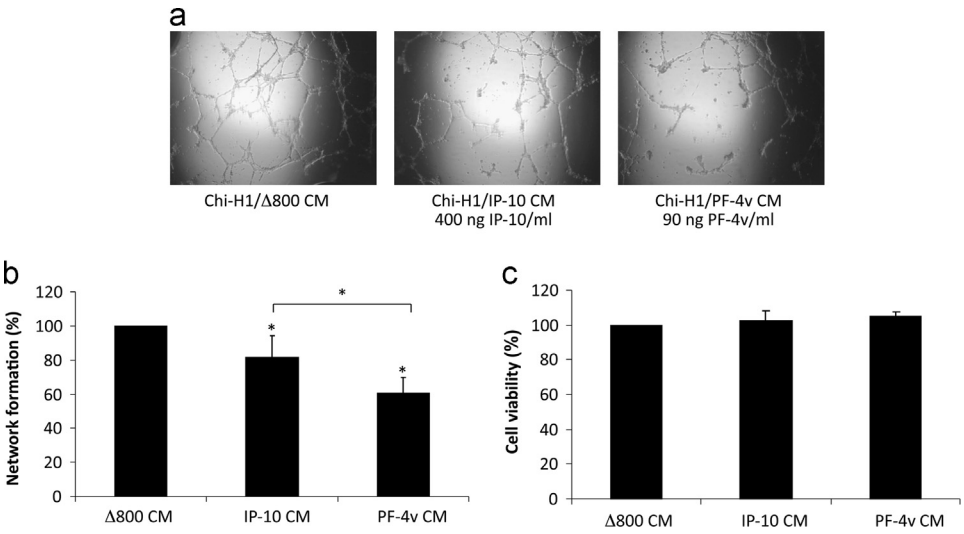

Fig. 6. Anti-angiogenic effects of CM from Chi-H1/PF-4var and Chi-H1/IP-10-infected KS-IMM cells. KS-IMM cells were seeded on Matrigel-coated dishes and incubated with the supernatants (CM) of Chi-H1/IP-10, Chi-H1/PF-4var or Chi-H1/Δ800-infected (MOI 12 RU/cell) KS-IMM cells. After 12–18 h incubation, the formation of a network of tube-like structures was examined. (a) Images were recorded at 4 × magnification. (b) Quantification of angiogenesis was performed by counting the number of tube-like structures obtained in the different conditions. The results are expressed as percentages of the control (CM from Chi-H1/Δ800-infected cells) and are the means ± SD from four independent experiments. $^{*}p=0{,}029$ in the Mann–Whitney Test. (c) The cell viability of KS-IMM cells after incubation with the different conditioned media was determined by MTT assay and is expressed as percentage of the control (Chi-H1/Δ800-infected cells).

non-infected cells. As depicted in Fig. 7, a vector dose-dependent specific decrease of the VEGF-A transcripts was observed in all infected cells, compared to the control, independently of vector arming with a transgene. At the MOI of 3 RU/cell, a 40% decrease of VEGF-A cDNA levels was observed compared to the uninfected control, which could be further enhanced to 50–60% by increasing the MOI to 12 or 24 RU/cell. The amounts of VEGF-A transcripts were normalized to those of 18S ribosomal RNA. The decrease of the levels of VEGF-A transcripts is unlikely to be due to cell killing upon viral infection. Indeed, transcription levels were not modified for the housekeeping gene GAPDH (data not shown), arguing for the specificity of VEGF-A expression inhibition upon parvovirus (vector) infection.

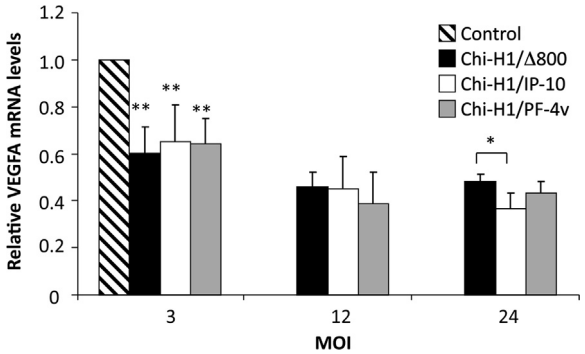

Fig. 7. Inhibition of VEGF-A expression in KS-IMM cells after parvoviral infection. 5×10^5 KS-IMM cells were infected with indicated viral vectors at increasing MOI, or mock-treated (control). At day 2 post-infection, total RNA was extracted from the cells and reverse transcribed. cDNAs were subjected to real time PCR using primers and probes specific for VEGF-A transcripts or 18S ribosomal RNA. VEGF-A mRNA relative abundances were determined using the ddCt method. dCt values were calculated using 18S ribosomal RNA as a reference sample, and then ddCt values were calculated relative to the control (non infected cells). Values are means from three independent experiments. $^{**}p < 0{,}01$; $^{*}p < 0{,}05$ in the Mann–Whitney test.

Discussion

Anti-angiogenic therapy has been recognized as a powerful potential strategy for impeding the growth of various tumors. However, despite the development of inhibitors of angiogenic signalling, in particular VEGF signalling, to control tumor neovascularization and growth, no major therapeutic effects have been observed to date. This is mainly because of the emergence of several resistance mechanisms that contribute to develop alternative angiogenic pathways or even to enhance tumor invasiveness, thereby circumventing anti-angiogenic therapy (Soda et al., 2013; Ebos and Kerbel, 2011; Giuliano and Pages, 2013). Thus, there is an urgent need to develop new approaches to overcome these limitations. Among alternative strategies to target tumor vasculature, some oncolytic viruses open up new prospects, as they selectively infect and destroy tumor vasculature while normal vasculature remains intact (Breitbach et al., 2011, 2013). Over the past years, experimental data have been accumulated on the potential of oncolytic parvoviruses for cancer therapy, leading to a phase I/IIa clinical trial of the rat parvovirus H-1PV in patients with recurrent glioblastoma multiforme (Rommelaere et al., 2010; Geletneky et al., 2012). The rodent parvoviruses are rarely pathogenic to host animals, and if so this effect is mainly restricted to fetuses and neonates (Jacoby et al., 1996). Typical features that parvoviruses may induce in neonates include leukopenia and hemorrhages of several tissues, suggesting that lymphocytes and vascular endothelium are among the main cellular targets of parvovirus infection (Jacoby et al., 1996). In this context, we specifically addressed the question whether the rodent parvovirus H-1PV can target endothelial cells *in vitro* and, if so, to which extent this property may contribute to its antitumor activity.

In this study we show that cultures of human normal (HUVEC) and immortalized (KS-IMM) endothelial cells sustain an abortive viral cycle upon infection with H-1PV and are sensitive to H-1PV cytotoxicity. In a xenograft KS model in mice, H-1PV infection of KS-IMM cells did not prevent tumor appearance but significantly inhibited tumor growth, resulting in a marked extension of animal survival. Although this effect can most likely be assigned to the oncotoxicity of the virus, other factors may contribute to H-1PV-mediated inhibition of KS-IMM tumor growth. In support of this possibility, parvovirus (vector) infection was found to specifically inhibit the expression of the key angiogenic molecule VEGF-A. VEGF-A is produced by KS-IMM cells and has been shown to

promote their growth *in vitro* and *in vivo* (Cornali et al., 1996; Masood et al., 1997). Members of the VEGF/VEGF receptor (VEGFR) family play critical roles in promoting tumor angiogenesis and constitute the main targets of anti-angiogenic therapies that have been developed so far (Kowanetz and Ferrara, 2006; Ebos and Kerbel, 2011). Recent reports show that oncolytic virus treatment results in tumor blood vessel coagulation and vasculature disruption (Breitbach et al., 2011, 2013) and may decrease the incidence of therapeutic resistance (Kirn and Thorne, 2009). It has been suggested that VEGF/VEGFR1/2 intracellular signalling may facilitate oncolytic virus infection/replication in tumor-associated endothelium (Kottke et al., 2010). Whether this also applies to H-1PV infection of KS-IMM tumors remains to be determined. The molecular mechanisms leading to the down-regulation of VEGF-A expression upon H-1PV infection need to be further investigated. The expression of VEGF-A is controlled by complex mechanisms. Indeed it is potently stimulated by growth factors, cellular stresses, oncogenes and a variety of cytokines (Hoeben et al., 2004; Pages and Pouyssegur, 2005). Notably, treatment of neuroendocrine tumor patients with interferon-alpha down-regulates the expression of VEGF and tumor angiogenesis (Rosewicz et al., 2004). Therefore the possible involvement of this pathway in H-1PV-induced inhibition of VEGF-A expression is certainly worth testing. Altogether, our data show that parvoviruses combine anti-angiogenic and oncolytic properties, making them promising tools to treat vascular and highly angiogenic tumours. Recombinant vectors based on parvoviruses H-1PV and MVMp have been designed to deliver immunostimulatory transgenes, and were shown to have an enhanced tumor-suppressor activity compared to the parental virus in some cancer models (Enderlin et al., 2009; Haag et al., 2000; Wetzel et al., 2007; Dempe et al., 2012). This prompted us to evaluate the impact of PV-mediated delivery of two angiostatic chemokines on KS-IMM cell viability, growth and angiogenic phenotype *in vitro*. Interestingly, the anti-angiogenic activity of H-1PV vectors expressing PF-4var or IP-10 revealed at least two components, one of which required direct KS-IMM cell infection with the vector, whereas the other was mediated by conditioned media from (vector)-infected cells. The former direct effect resulted from the lytic activity of the virus (vector) on endothelial cells, irrespective of transgene-arming. The latter indirect effect was mediated by transduced chemokines and consisted of the reduction of endothelial cell growth and the inhibition of their angiogenic (tube-forming) phenotype. Several mechanisms have been reported to contribute to the angiostatic activity of PF-4/CXCL4 (Vandercappellen et al., 2011 and references therein). In particular PF-4 competes for FGF-2 or VEGF binding (Jouan et al., 1999), interacts with VEGF, and disrupts VEGF receptor signaling (Gengrinovitch et al., 1995). As stated above, the stimulation of endothelial cell-specific growth factor signaling pathways at the tumor site may provide a favourable milieu to initiate replication of oncolytic viruses (Breitbach et al., 2013; Kottke et al., 2010). If this also applies to parvovirus H-1PV, one may speculate that, at a later stage, the direct toxic activity of PF-4var/IP-10-transducing parvoviral vectors acts overridden by the concurrent anti-angiogenic effects of the chemokines in tumor-associated endothelial cells. The activity of IP-10 and PF-4var is mediated via a common receptor, CXCR3 (Struyf et al., 2011; Loetscher et al., 1996). The influence of CXCR3 signaling on tumour progression is controversial, both promoting and inhibiting effects have been reported (Struyf et al., 2007; Vandercappellen et al., 2011; Kawada et al., 2007; Liu et al., 2010, 2011; Wu et al., 2012; Sato et al., 2007). Besides inhibiting angiogenesis, CXCR3 ligands recruit CXCR3-expressing T and NK cells (Keeley et al., 2011 and references therein). CXCR3 exists in three isoforms, CXCR3A, CXCR3B and CXCR3-alt which are generated through alternative splicing (Ehlert et al., 2004). CXCR3A is involved in the recruitment of activated T and NK cells (Mueller et al., 2008), while CXCR3B is believed to mediate the angiostatic activity of PF-4/PF-4var, IP-10, Mig/CXCL9 and I-TAC/CXCL11 on endothelial cells (Lasagni et al., 2003; Struyf et al., 2011). In this paper we show that, as expected, CXCR3 is expressed on KS-IMM cells, and that expression of this receptor is not modified by parvovirus infection. Whether treatment of KS-IMM tumors with recombinant parvoviruses expressing IP-10 and PF-4var may improve the anti-cancer activity of wild-type H-1PV in recipient mice remains to be determined. Previous studies from our laboratory using two syngeneic tumor models of vascularized tumors, (hemangiosarcoma and glioblastoma), have shown that parvovirus MVMp vector-mediated expression of IP-10, either alone (Giese et al., 2002) or in combination with TNF-α (Enderlin et al., 2009), significantly increased the survival of recipient mice. However no evidence of a significant inhibition of tumor vascularization could be shown in these models, and chemokine-mediated immunostimulation was most likely responsible for the therapeutic efficacy of IP-10-expressing MVMp.

In conclusion, our data argue for the ability of H-1PV to inhibit tumor angiogenesis, by showing that at least under *in vitro* conditions the virus can directly kill infected endothelial cells, and also act in an indirect way by inhibiting the expression of the key angiogenic factor VEGF. This possibility cannot be tested readily using a tumor model in mice, since mouse cells (including endothelial ones) are restricted in their permissiveness to the rat parvovirus H-1PV due to blocking of the virus cycle at an early step of infection (Wrzesinski et al., 2003). This resistance of the mouse vasculature to H-1PV infection may limit the efficiency of H-1PV against KS-IMM tumor xenografts into mice. However, the intrinsic endothelial nature of the KS tumor allowed to demonstrate the anti-angiogenic effects of the virus under conditions in which target cells are proliferating *in vivo*. Furthermore, our data indicate that H-1PV can be used as a vector to transduce tumor cells with functionally active chemokines endowed with anti-angiogenesis properties. Taken together, this evidence warrants the further validation of H-1PV for the treatment of highly vascularized tumors.

Material and methods

Cells and reagents

The simian virus 40 (SV40)-transformed human newborn kidney cells NB-324K (Tattersall and Bratton, 1983) were propagated in Eagle's minimal essential medium (MEM, Sigma-Aldrich, Taufkirchen, Germany) supplemented with 5% fetal bovine serum (FBS, PAA Laboratories, Pasching, Austria), 2 mM L-glutamine (Gibco/Invitrogen, Karlsruhe, Germany) and antibiotics (100 U/ml of penicillin G and 100 μg/ml of streptomycin sulphate, Gibco/Invitrogen).

Primary human umbilical vein endothelial cells (HUVEC) were purchased from, Promocell (Heidelberg, Germany) and cultured in endothelial basal (EBM-2) medium supplemented with the EGM-2 Bulletkit (Lonza, Cologne, Germany).

The simian virus 40T antigen-, adenovirus 5-transformed human cell line 293T/17 was obtained from the American Type Culture Collection. The Kaposi sarcoma cell line, KS-IMM (Albini et al., 1997), was kindly provided by A.Vecchi (Istituto Clinico Humanitas, Rozzano, Italy). The 293T/17 and KS-IMM cells were grown in Dulbecco's modified Eagle's medium (DMEM, Sigma-Aldrich) supplemented with 10% fetal bovine serum, 2 mM L-glutamine and antibiotics.

Plasmids

The H-1PV parvoviral based vectors pChi-H1/Δ800 and pChi-H1/IP-10 have been described elsewhere (Dempe et al., 2012).

Table 1
Primers and probes used for cDNA amplification and detection.

Target gene[a]	Primer/probe sequence (5′→3′)	$T_{an.}$ (°C)	Amplicon size (bp)
h GAPDH	GCCTTCCGTGTCCCCACTGC[1] GGCTGGTGGTCCAGGGGTCT[2]	62	334
PV NS1	CTAAATGGAAAGGACATCGGTTGGAATAG[1] GCCTCCGTCCCTTGGTGG[2]	62	570
h CXCR3	GGTGAGTGACCACCAAGTGC[1] AGGTAGCGGTCAAAGCTGATGC[2]	61	441
h VEGF-A	CCATGAACTTTCTGCTGTCTTG[1] TGAACTTCACCACTTCGTGAT[2] 6FAM/TGCTCTACC/ZEN/TCCACCATGCCAAG/IABkFQ[3]	60	131
h RN18S1	ACGGACAGGATTGACAGATTG[1] ATCGCTCCACCAACTAAGAAC[2] 6FAM/ACCACCCAC/ZEN/GGAATCGAGAAAGAG/IABkFQ[3]	60	80

$T_{an.}$ annealing temperature, bp base pairs, PV parvovirus, h human, GAPDH glyceraldehyde-3-phosphate dehydrogenase, RN18S1 18S ribosomal 1 RNA.

[a] Target cDNAs were amplified with the indicated pair of forward[1] and reverse[2] primers. Relative transcripts expression level was determined by TaqMan real time PCR using indicated probes[3], labeled with the reporter dye 6-carboxyfluorescein (6FAM) at the 5′ end, with the quencher dye Iowa Black FQ (IABkFQ) at the 3′ end and the ZEN internal quencher.

pChi-H1/PF-4var was obtained by PCR amplification of the PF-4var cDNA from the pHENI expression vector (Struyf et al., 2007) with primers containing NotI-XmaI linkers and cloned in the NotI-XmaI sites of the multiple cloning site of the pChi-H1/Δ800 vector.

Virus infection, production and titration

Virus infections were performed at 37 °C for 1 h with a virus inoculum of purified (recombinant) H-1PV and occasional rocking of the plate. Stocks of recombinants H-1PV were produced by transfection of 293T cells and wild-type (wt) H-1PV by infection of NB-324K cells, purified by iodixanol gradient centrifugation and titrated by infected cell hybridization assay (recombinant and wt H-1PV) or plaque assay (wt H-1PV) on NB-324K indicator cells as previously described (Haag et al., 2000; Tattersall and Bratton, 1983). Wt H-1PV titers were previously shown to be similar, whether determined using the infected cell hybridization assay or the plaque assay (Haag et al., 2000). Virus titers were expressed as replication units (RU) or plaque forming units (PFU) per milliliter of virus suspension.

Quantification of transgene secretion

Levels of secreted cytokines were measured in the cell culture supernatants of recombinant H-1PV-infected KS-IMM and HUVEC cells at different time-points post-infection (p.i.) using specific ELISAs for IP-10 (Abu El-Asrar et al., 2004), PF-4var (Vandercappellen et al., 2007) and VEGF-A (BIOO Scientific, Austin, TX).

Immunoblotting

A 1–2 × 10^6 cells were infected with H-1PV at a MOI of 3 RU/cell and harvested at different times p.i. After cell lysis in RIPA buffer (150 mM NaCl, 10 mM Tris, 1 mM EDTA, 1% NP-40, 0.5% sodium deoxycholate, 0.1% SDS, protease inhibitor) and protein quantification (Bio-Rad Protein Assay, BioRad Laboratories, Munich, Germany), 20 μg of total proteins were separated by SDS-10% polyacrylamide gel electrophoresis (SDS-PAGE) and electro-transferred to Protran nitrocellulose membranes (PerkinElmer Life Sciences, Überlingen, Germany). The membranes were incubated with either rabbit polyclonal antiserum directed against NS1 (SP8, Brockhaus et al., 1996), NS2 (α-NS2p, Wrzesinski et al., 2003), H-1PV capsid proteins (α-VP, Kestler et al., 1999) and the appropriate horseradish peroxidase-coupled antibody (Promega, Mannheim, Germany).or mouse monoclonal anti-14-3-3 β-horseradish peroxidase-coupled antibody (H-8, Santa Cruz Biotechnology, Santa Cruz, CA). Immunoreactive proteins were revealed by enhanced chemiluminescence (GE Healthcare Europe, Freiburg, Germany).

Southern blot analysis

Low molecular weight viral DNA was extracted from infected cells using the DNeasy Blood and Tissue kit (Qiagen, Hilden, Germany) according to the manufacturer's instructions. Viral replicative DNA forms were separated by 1% agarose gel electrophoresis. After gel denaturation in a 1.5 M NaCl, 0.5 M NaOH solution and neutralization in a 1.5 M NaCl, 0.5 M Tris–HCl pH7.2, 1 mM EDTA solution, DNA molecules were transferred onto nitrocellulose membranes (Protran, GE Healthcare) for 15–20 h at room temperature by capillary action in the presence of 10X SSC buffer (1.5 M NaCl, 0.15 M sodium citrate) and further linked to the membrane by heat treatment for 2 h at 80 °C. Membranes were hybridized at 65 °C with a 1000bp-long ^{32}P-labelled H-1PV DNA probe from the NS region and exposed to autoradiographic films (Biomax, MS Film Kodak, Kiel, Germany) at −80 °C with intensifier screen.

Assessment of cell viability and cell lysis

Cell viability was tested with the 3-(4,5-dimethylthiazol-2-yl)-2,5-diphenyltetrazolium bromide (MTT) assay as recommended by the manufacturer (Sigma-Aldrich). A 1.5 × 10^4 (KS-IMM) or 2 × 10^4 (HUVEC) cells per well were cultured in 48-well plates and infected with (recombinant) H-1PV at different MOIs. At day 3 post infection, MTT 5 μg/ml (final concentration) was added to the cell culture medium and cells were incubated 4 h at 37 °C. After removing the supernatant and drying the cells, 100 μl of isopropanol were added. The absorbance was measured at 595 nm (Multiscan PlusTM, Titertek Instruments, Huntsville, AL).

Cell lysis was determined by the release of lactate dehydrogenase (LDH) into the culture medium by using the Cytotox 96 cytotoxicity assay kitTM (Promega) according to the manufacturer's instructions.

RT-PCR analysis and quantitative real time PCR

Total RNA was extracted from cells using the RNEasy kit (Qiagen). About 1–2 μg of total RNA was treated with DNAse I, reverse-transcribed using 200 U of RNA-dependent DNA polymerase M-MLV RT (Promega) in the presence of 500 μM dNTPs (Invitrogen), 20 U of RNasin and 20 ng/μl of random primers (Promega) in a reaction volume of 25 μl for 1 h at 38 °C. After heat-inactivation of the reverse-transcriptase, the cDNA was diluted 1:8 in RNAse/DNAse-free water (Invitrogen). Specific PCR amplifications were performed in 25 μl reactions using 5 μl of cDNA, 200 μM of dNTPs (Invitrogen), 1.5 mM of $MgCl_2$ (Invitrogen), 500 nM of each specific forward and reverse primers (Eurofins MWG Operon, Ebersberg, Germany) and 2 U of Taq DNA polymerase (Invitrogen). The PCR cycles were performed as following: 95 °C, 3 min for initial

denaturation, 35 cycles of 95 °C, 30 s, annealing: 53–60 °C, 30 s, extension:72 °C, 30 s and 72 °C, 7 min, for the final extension.

The relative transcript levels were determined by TaqMan real time PCR using the primers and probes listed in Table 1. Quantitative PCR was performed with 4 μl of cDNA, 10 μl of 2 × Taqman PCR master mix (Perkin-Elmer Applied Biosystems, Rodgau, Germany), 250 nM of each primer and probe in a total volume of 20 μl. The thermal cycling conditions were performed as following: 50 °C, 2 min, 95 °C, 10 min, followed by 45 cycles of 95 °C, 15 s and 60 °C, 1 min. Data collection was performed during each annealing phase. Appropriate controls were included in each PCR reaction. The relative abundance of transcripts was determined by the ddCt method. dCt values were calculated using 18S ribosomal RNA as a reference sample, and the ddCt values relative to the control gene (from mock-infected cells).

In vitro angiogenesis assay

The tube-like formation assay was performed following the manufacturer's instructions (*In vitro* angiogenesis assay kit, Millipore, Schwalbach, Germany). Briefly, wells from a 96-well plate were coated with ECMatrix solution and incubated for 1 h at 37 °C to allow the matrix solution to solidify. A 3×10^3 KS-IMM cells were seeded in each well and incubated with the supernatants of recombinant virus-infected cells. Tube formation was monitored under an inverted microscope 12–18 h after seeding. The number of tubular structures formed in each condition was determined in 10 fields using the freeware ImageJ. Cell viability was determined by MTT assay in the different conditioned media and expressed as percentage of control (conditioned medium of Chi-H1/Δ800-infected KS-IMM cells).

Tumor model

Female nude Balb/c mice (Janvier Labs, St Berthevin, France), 7–8 weeks old were maintained under pathogen-free conditions. KS-IMM cells were mock (buffer)-treated or infected with H-1PV at a MOI of 12 RU/cell. At 4 h post-infection, 3×10^6 KS-IMM cells suspended in ice-cold calcium-, magnesium- and glucose-containing Dulbecco's PBS were mixed with liquid Matrigel (BD Biosciences, Heidelberg, Germany) to a final volume of 200 μl. The mixture was subcutaneously (s.c.) implanted into the right flank of mice (7–13 mice/group). Tumor sizes were measured with an electronic digital calliper (Farnell, Germany) three times a week and the tumor volume was calculated according to the formula: $V = 1/2 \times \text{length} \times \text{width}^2$ (mm^3). Animals were killed for ethical reasons when the tumor volume reached 1500 mm^3. The animal experimental procedures were approved by the responsible Animal Protection Officer at the DKFZ and by the Regional Council according to the German Protection Law.

Statistical analysis

Statistically significant differences were determined by the nonparametric Mann–Whitney rank sum test. Differences were considered significant at $p \leq 0.05$.

Acknowledgments

We are grateful to Annunciata Vecchi and Marina Sironi for kindly providing the KS-IMM cells, Nathalie Salomé for NS1 and NS2 antibodies and critical reading of the manuscript and Sebastian Dempe for his help in the construction of viral vectors. We especially thank Isabelle Ronsse for excellent technical assistance, Renate Geibig for her help in animal work and Nicolas Jauniaux for assistance in editing the figures. This work was supported by the Fund for Scientific Research of Flanders (FWO-Vlaanderen project G.0773.13, Belgium) and the Interuniversity Attraction Poles Programme initiated by the Belgian Science Policy Office (I.A.P. project P7/40).

References

Abu El-Asrar, A.M., Struyf, S., Descamps, F.J., Al-Obeidan, S.A., Proost, P., Van Damme, J., Opdenakker, G., Geboes, K., 2004. Chemokines and gelatinases in the aqueous humor of patients with active uveitis. Am. J. Ophthalmol. 138 (3), 401–411.

Albini, A., Paglieri, I., Orengo, G., Carlone, S., Aluigi, M.G., DeMarchi, R., Matteucci, C., Mantovani, A., Carozzi, F., Donini, S., Benelli, R., 1997. The beta-core fragment of human chorionic gonadotrophin inhibits growth of Kaposi's sarcoma-derived cells and a new immortalized Kaposi's sarcoma cell line. AIDS 11 (6), 713–721.

Angelova, A.L., Aprahamian, M., Balboni, G., Delecluse, H.J., Feederle, R., Kiprianova, I., Grekova, S.P., Galabov, A.S., Witzens-Harig, M., Ho, A.D., Rommelaere, J., Raykov, Z., 2009. Oncolytic rat parvovirus H-1PV, a candidate for the treatment of human lymphoma: *in vitro* and *in vivo* studies. Mol. Ther. 17 (7), 1164–1172.

Angiolillo, A.L., Sgadari, C., Taub, D.D., Liao, F., Farber, J.M., Maheshwari, S., Kleinman, H.K., Reaman, G.H., Tosato, G., 1995. Human interferon-inducible protein 10 is a potent inhibitor of angiogenesis *in vivo*. J. Exp. Med. 182 (1), 155–162.

Ball-Goodrich, L.J., Leland, S.E., Johnson, E.A., Paturzo, F.X., Jacoby, R.O., 1998. Rat parvovirus type 1: the prototype for a new rodent parvovirus serogroup. J. Virol. 72 (4), 3289–3299.

Bergers, G., Song, S., Meyer-Morse, N., Bergsland, E., Hanahan, D., 2003. Benefits of targeting both pericytes and endothelial cells in the tumor vasculature with kinase inhibitors. J. Clin. Invest. 111 (9), 1287–1295.

Bhat, R., Dempe, S., Dinsart, C., Rommelaere, J., 2011. Enhancement of NK cell antitumor responses using an oncolytic parvovirus. Int. J. Cancer 128 (4), 908–919.

Bodnar, R.J., Yates, C.C., Wells, A., 2006. IP-10 blocks vascular endothelial growth factor-induced endothelial cell motility and tube formation via inhibition of calpain. Circ. Res. 98 (5), 617–625.

Brandenburger, A., Legendre, D., Avalosse, B., Rommelaere, J., 1990. NS-1 and NS-2 proteins may act synergistically in the cytopathogenicity of parvovirus MVMp. Virology 174 (2), 576–584.

Breitbach, C.J., Arulanandam, R., De Silva, N., Thorne, S.H., Patt, R., Daneshmand, M., Moon, A., Ilkow, C., Burke, J., Hwang, T.H., Heo, J., Cho, M., Chen, H., Angarita, F. A., Addison, C., McCart, J.A., Bell, J.C., Kirn, D.H., 2013. Oncolytic vaccinia virus disrupts tumor-associated vasculature in humans. Cancer Res. 73 (4), 1265–1275.

Breitbach, C.J., Thorne, S.H., Bell, J.C., Kirn, D.H., 2011. Targeted and armed oncolytic poxviruses for cancer: the lead example of JX-594. Curr. Pharmacol. Biotechnol. 13 (9), 1768–1772.

Brockhaus, K., Plaza, S., Pintel, D.J., Rommelaere, J., Salome, N., 1996. Nonstructural proteins NS2 of minute virus of mice associate *in vivo* with 14-3-3 protein family members. J. Virol. 70 (11), 7527–7534.

Caillet-Fauquet, P., Perros, M., Brandenburger, A., Spegelaere, P., Rommelaere, J., 1990. Programmed killing of human cells by means of an inducible clone of parvoviral genes encoding non-structural proteins. EMBO J. 9 (9), 2989–2995.

Chung, A.S., Lee, J., Ferrara, N., 2010. Targeting the tumour vasculature: insights from physiological angiogenesis. Nat. Rev. Cancer 10 (7), 505–514.

Cole, C.A., Nathanson, N., Rivet, H., 1970. Viral hemorrhagic encephalopathy of rats. II. Pathogenesis of central nervous system lesions. Am. J. Epidemiol. 91 (3), 339–350.

Cornali, E., Zietz, C., Benelli, R., Weninger, W., Masiello, L., Breier, G., Tschachler, E., Albini, A., Sturzl, M., 1996. Vascular endothelial growth factor regulates angiogenesis and vascular permeability in Kaposi's sarcoma. Am. J. Pathol. 149 (6), 1851–1869.

Cornelis, J.J., Spruyt, N., Spegelaere, P., Guetta, E., Darawshi, T., Cotmore, S.F., Tal, J., Rommelaere, J., 1988. Sensitization of transformed rat fibroblasts to killing by parvovirus minute virus of mice correlates with an increase in viral gene expression. J. Virol. 62 (9), 3438–3444.

Cotmore, S.F., D'Abramo Jr., A.M., Carbonell, L.F., Bratton, J., Tattersall, P., 1997. The NS2 polypeptide of parvovirus MVM is required for capsid assembly in murine cells. Virology 231 (2), 267–280.

Cotmore, S.F., Gottlieb, R.L., Tattersall, P., 2007. Replication initiator protein NS1 of the parvovirus minute virus of mice binds to modular divergent sites distributed throughout duplex viral DNA. J. Virol. 81 (23), 13015–13027.

Cotmore, S.F., Tattersall, P., 2007. Parvoviral host range and cell entry mechanisms. Adv. Virus Res. 70, 183–232.

Dempe, S., Lavie, M., Struyf, S., Bhat, R., Verbeke, H., Paschek, S., Berghmans, N., Geibig, R., Rommelaere, J., Van Damme, J., Dinsart, C., 2012. Antitumoral activity of parvovirus-mediated IL-2 and MCP-3/CCL7 delivery into human pancreatic cancer: implication of leucocyte recruitment. Cancer Immunol. Immunother. 61 (11), 2113–2123.

Dubrac, A., Quemener, C., Lacazette, E., Lopez, F., Zanibellato, C., Wu, W.G., Bikfalvi, A., Prats, H., 2010. Functional divergence between 2 chemokines is conferred by single amino acid change. Blood 116 (22), 4703–4711.

Ebos, J.M., Kerbel, R.S., 2011. Antiangiogenic therapy: impact on invasion, disease progression, and metastasis. Nat. Rev. Clin. Oncol. 8 (4), 210–221.

Ehlert, J.E., Addison, C.A., Burdick, M.D., Kunkel, S.L., Strieter, R.M., 2004. Identification and partial characterization of a variant of human CXCR3 generated by posttranscriptional exon skipping. J. Immunol. 173 (10), 6234–6240.
Eisman, R., Surrey, S., Ramachandran, B., Schwartz, E., Poncz, M., 1990. Structural and functional comparison of the genes for human platelet factor 4 and PF4alt. Blood 76 (2), 336–344.
Ellis, L.M., Hicklin, D.J., 2008. VEGF-targeted therapy: mechanisms of anti-tumour activity. Nat. Rev. Cancer 8 (8), 579–591.
Enderlin, M., Kleinmann, E.V., Struyf, S., Buracchi, C., Vecchi, A., Kinscherf, R., Kiessling, F., Paschek, S., Sozzani, S., Rommelaere, J., Cornelis, J.J., Van Damme, J., Dinsart, C., 2009. TNF-alpha and the IFN-gamma-inducible protein 10 (IP-10/CXCL-10) delivered by parvoviral vectors act in synergy to induce antitumor effects in mouse glioblastoma. Cancer Gene Ther. 16 (2), 149–160.
Farber, J.M., 1997. Mig and IP-10: CXC chemokines that target lymphocytes. J. Leukoc. Biol. 61 (3), 246–257.
Ferrara, N., 2010. Pathways mediating VEGF-independent tumor angiogenesis. Cytokine Growth Factor Rev. 21 (1), 21–26.
Ferrara, N., Alitalo, K., 1999. Clinical applications of angiogenic growth factors and their inhibitors. Nat. Med. 5 (12), 1359–1364.
Geletneky, K., Huesing, J., Rommelaere, J., Schlehofer, J.R., Leuchs, B., Dahm, M., Krebs, O., von Knebel Doeberitz, M., Huber, B., Hajda, J., 2012. Phase I/IIa study of intratumoral/intracerebral or intravenous/intracerebral administration of Parvovirus H-1 (ParvOryx) in patients with progressive primary or recurrent glioblastoma multiforme: ParvOryx01 protocol. BMC Cancer 12, 99.
Geletneky, K., Kiprianova, I., Ayache, A., Koch, R., Herrero, Y.C.M., Deleu, L., Sommer, C., Thomas, N., Rommelaere, J., Schlehofer, J.R., 2010. Regression of advanced rat and human gliomas by local or systemic treatment with oncolytic parvovirus H-1 in rat models. Neuro Oncol. 12 (8), 804–814.
Gengrinovitch, S., Greenberg, S.M., Cohen, T., Gitay-Goren, H., Rockwell, P., Maione, T.E., Levi, B.Z., Neufeld, G., 1995. Platelet factor-4 inhibits the mitogenic activity of VEGF121 and VEGF165 using several concurrent mechanisms. J. Biol. Chem. 270 (25), 15059–15065.
Gerwins, P., Skoldenberg, E., Claesson-Welsh, L., 2000. Function of fibroblast growth factors and vascular endothelial growth factors and their receptors in angiogenesis. Crit. Rev. Oncol. Hematol. 34 (3), 185–194.
Giese, N.A., Raykov, Z., DeMartino, L., Vecchi, A., Sozzani, S., Dinsart, C., Cornelis, J.J., Rommelaere, J., 2002. Suppression of metastatic hemangiosarcoma by a parvovirus MVMp vector transducing the IP-10 chemokine into immunocompetent mice. Cancer Gene Ther. 9 (5), 432–442.
Giuliano, S., Pages, G., 2013. Mechanisms of resistance to anti-angiogenesis therapies. Biochimie 95 (6), 1110–1119.
Green, C.J., Charles, R.S., Edwards, B.F., Johnson, P.H., 1989. Identification and characterization of PF4varl, a human gene variant of platelet factor 4. Mol. Cell. Biol. 9 (4), 1445–1451.
Grekova, S.P., Rommelaere, J., Raykov, Z., 2012. Parvoviruses-tools to fine-tune anticancer immune responses. Oncoimmunology 1 (8), 1417–1419.
Haag, A., Menten, P., Van Damme, J., Dinsart, C., Rommelaere, J., Cornelis, J.J., 2000. Highly efficient transduction and expression of cytokine genes in human tumor cells by means of autonomous parvovirus vectors; generation of antitumor responses in recipient mice. Hum. Gene Ther. 11 (4), 597–609.
Hoeben, A., Landuyt, B., Highley, M.S., Wildiers, H., Van Oosterom, A.T., De Bruijn, E. A., 2004. Vascular endothelial growth factor and angiogenesis. Pharmacol. Rev. 56 (4), 549–580.
Jacoby, R.O., Ball-Goodrich, L.J., Besselsen, D.G., McKisic, M.D., Riley, L.K., Smith, A.L., 1996. Rodent parvovirus infections. Lab. Anim. Sci. 46 (4), 370–380.
Jacoby, R.O., Johnson, E.A., Paturzo, F.X., Ball-Goodrich, L., 2000. Persistent rat virus infection in smooth muscle of euthymic and athymic rats. J. Virol. 74 (24), 11841–11848.
Jouan, V., Canron, X., Alemany, M., Caen, J.P., Quentin, G., Plouet, J., Bikfalvi, A., 1999. Inhibition of *in vitro* angiogenesis by platelet factor-4-derived peptides and mechanism of action. Blood 94 (3), 984–993.
Kawada, K., Hosogi, H., Sonoshita, M., Sakashita, H., Manabe, T., Shimahara, Y., Sakai, Y., Takabayashi, A., Oshima, M., Taketo, M.M., 2007. Chemokine receptor CXCR3 promotes colon cancer metastasis to lymph nodes. Oncogene 26 (32), 4679–4688.
Keeley, E.C., Mehrad, B., Strieter, R.M., 2011. Chemokines as mediators of tumor angiogenesis and neovascularization. Exp. Cell. Res. 317 (5), 685–690.
Keeley, E.C., Mehrad, B., Strieter, R.M., 2010. CXC chemokines in cancer angiogenesis and metastases. Adv. Cancer Res. 106, 91–111.
Kestler, J., Neeb, B., Struyf, S., Van Damme, J., Cotmore, S.F., D'Abramo, A., Tattersall, P., Rommelaere, J., Dinsart, C., Cornelis, J.J., 1999. cis requirements for the efficient production of recombinant DNA vectors based on autonomous parvoviruses. Hum. Gene Ther. 10 (10), 1619–1632.
Kirn, D.H., Thorne, S.H., 2009. Targeted and armed oncolytic poxviruses: a novel multi-mechanistic therapeutic class for cancer. Nat. Rev. Cancer 9 (1), 64–71.
Kottke, T., Hall, G., Pulido, J., Diaz, R.M., Thompson, J., Chong, H., Selby, P., Coffey, M., Pandha, H., Chester, J., Melcher, A., Harrington, K., Vile, R., 2010. Antiangiogenic cancer therapy combined with oncolytic virotherapy leads to regression of established tumors in mice. J. Clin. Invest. 120 (5), 1551–1560.
Kowanetz, M., Ferrara, N., 2006. Vascular endothelial growth factor signaling pathways: therapeutic perspective. Clin. Cancer Res. 12 (17), 5018–5022.
Lasagni, L., Francalanci, M., Annunziato, F., Lazzeri, E., Giannini, S., Cosmi, L., Sagrinati, C., Mazzinghi, B., Orlando, C., Maggi, E., Marra, F., Romagnani, S., Serio, M., Romagnani, P., 2003. An alternatively spliced variant of CXCR3 mediates the inhibition of endothelial cell growth induced by IP-10, Mig, and I-TAC, and acts as functional receptor for platelet factor 4. J. Exp. Med. 197 (11), 1537–1549.
Li, X., Rhode 3rd, S.L., 1990. Mutation of lysine 405 to serine in the parvovirus H-1 NS1 abolishes its functions for viral DNA replication, late promoter trans activation, and cytotoxicity. J. Virol. 64 (10), 4654–4660.
Liu, C., Luo, D., Reynolds, B.A., Meher, G., Katritzky, A.R., Lu, B., Gerard, C.J., Bhadha, C.P., Harrison, J.K., 2010. Chemokine receptor CXCR3 promotes growth of glioma. Carcinogenesis 32 (2), 129–137.
Liu, M., Guo, S., Stiles, J.K., 2011. The emerging role of CXCL10 in cancer (Review). Oncol. Lett. 2 (4), 583–589.
Loetscher, M., Gerber, B., Loetscher, P., Jones, S.A., Piali, L., Clark-Lewis, I., Baggiolini, M., Moser, B., 1996. Chemokine receptor specific for IP10 and mig: structure, function, and expression in activated T-lymphocytes. J. Exp. Med. 184 (3), 963–969.
Lorson, C., Burger, L.R., Mouw, M., Pintel, D.J., 1996. Efficient transactivation of the minute virus of mice P38 promoter requires upstream binding of NS1. J. Virol. 70 (2), 834–842.
Margolis, G., Kilham, L., 1970. Parvovirus infections, vascular endothelium, and hemorrhagic encephalopathy. Lab. Invest. 22 (5), 478–488.
Masood, R., Cai, J., Zheng, T., Smith, D.L., Naidu, Y., Gill, P.S., 1997. Vascular endothelial growth factor/vascular permeability factor is an autocrine growth factor for AIDS-Kaposi sarcoma. Proc. Nat. Acad. Sci. U.S.A. 94 (3), 979–984.
McKisic, M.D., Macy Jr., J.D., Delano, M.L., Jacoby, R.O., Paturzo, F.X., Smith, A.L., 1998. Mouse parvovirus infection potentiates allogeneic skin graft rejection and induces syngeneic graft rejection. Transplantation 65 (11), 1436–1446.
Mesri, E.A., Cesarman, E., Boshoff, C., 2010. Kaposi's sarcoma and its associated herpesvirus. Nat. Rev. Cancer 10 (10), 707–719.
Moehler, M., Zeidler, M., Schede, J., Rommelaere, J., Galle, P.R., Cornelis, J.J., Heike, M., 2003. Oncolytic parvovirus H1 induces release of heat-shock protein HSP72 in susceptible human tumor cells but may not affect primary immune cells. Cancer Gene Ther. 10 (6), 477–480.
Moehler, M.H., Zeidler, M., Wilsberg, V., Cornelis, J.J., Woelfel, T., Rommelaere, J., Galle, P.R., Heike, M., 2005. Parvovirus H-1-induced tumor cell death enhances human immune response *in vitro* via increased phagocytosis, maturation, and cross-presentation by dendritic cells. Hum. Gene Ther. 16 (8), 996–1005.
Momoeda, M., Wong, S., Kawase, M., Young, N.S., Kajigaya, S., 1994. A putative nucleoside triphosphate-binding domain in the nonstructural protein of B19 parvovirus is required for cytotoxicity. J. Virol. 68 (12), 8443–8446.
Mueller, A., Meiser, A., McDonagh, E.M., Fox, J.M., Petit, S.J., Xanthou, G., Williams, T. J., Pease, J.E., 2008. CXCL4-induced migration of activated T lymphocytes is mediated by the chemokine receptor CXCR3. J. Leukoc. Biol. 83 (4), 875–882.
Narvaiza, I., Mazzolini, G., Barajas, M., Duarte, M., Zaratiegui, M., Qian, C., Melero, I., Prieto, J., 2000. Intratumoral coinjection of two adenoviruses, one encoding the chemokine IFN-gamma-inducible protein-10 and another encoding IL-12, results in marked antitumoral synergy. J. Immunol. 164 (6), 3112–3122.
Nuesch, J.P., Bar, S., Rommelaere, J., 2008. Viral proteins killing tumor cells: new weapons in the fight against cancer. Cancer Biol. Ther. 7 (9), 1374–1376.
Nuesch, J.P., Lacroix, J., Marchini, A., Rommelaere, J., 2012. Molecular pathways: rodent parvoviruses—mechanisms of oncolysis and prospects for clinical cancer treatment. Clin. Cancer Res. 18 (13), 3516–3523.
Pages, G., Pouyssegur, J., 2005. Transcriptional regulation of the vascular endothelial growth factor gene—a concert of activating factors. Cardiovasc. Res. 65 (3), 564–573.
Rommelaere, J., Cornelis, J.J., 1991. Antineoplastic activity of parvoviruses. J. Virol. Methods 33 (3), 233–251.
Rommelaere, J., Geletneky, K., Angelova, A.L., Daeffler, L., Dinsart, C., Kiprianova, I., Schlehofer, J.R., Raykov, Z., 2010. Oncolytic parvoviruses as cancer therapeutics. Cytokine Growth Factor Rev. 21 (2–3), 185–195.
Rosewicz, S., Detjen, K., Scholz, A., von Marschall, Z., 2004. Interferon-alpha: regulatory effects on cell cycle and angiogenesis. Neuroendocrinology 80 (Suppl. 1), 85–93.
Rubenstein, J.L., Kim, J., Ozawa, T., Zhang, M., Westphal, M., Deen, D.F., Shuman, M. A., 2000. Anti-VEGF antibody treatment of glioblastoma prolongs survival but results in increased vascular cooption. Neoplasia 2 (4), 306–314.
Sato, E., Fujimoto, J., Toyoki, H., Sakaguchi, H., Alam, S.M., Jahan, I., Tamaya, T., 2007. Expression of IP-10 related to angiogenesis in uterine cervical cancers. Br. J. Cancer 96 (11), 1735–1739.
Sieben, M., Schafer, P., Dinsart, C., Galle, P.R., Moehler, M., 2012. Activation of the human immune system via toll-like receptors by the oncolytic parvovirus H-1. Int. J. Cancer 132 (11), 2548–2556.
Siegl, G, 1984. Biology and pathogenicity of autonomous parvoviruses. In: B., K.I. (Ed.), The Parvoviruses. Plenum Publishing Corp., New York, pp. 297–362.
Soda, Y., Myskiw, C., Rommel, A., Verma, I.M., 2013. Mechanisms of neovascularization and resistance to anti-angiogenic therapies in glioblastoma multiforme. J. Mol. Med. (Berlin) 91 (4), 439–448.
Sodhi, A., Montaner, S., Patel, V., Zohar, M., Bais, C., Mesri, E.A., Gutkind, J.S., 2000. The Kaposi's sarcoma-associated herpes virus G protein-coupled receptor up-regulates vascular endothelial growth factor expression and secretion through mitogen-activated protein kinase and p38 pathways acting on hypoxia-inducible factor 1alpha. Cancer Res. 60 (17), 4873–4880.
Strieter, R.M., Burdick, M.D., Gomperts, B.N., Belperio, J.A., Keane, M.P., 2005. CXC chemokines in angiogenesis. Cytokine Growth Factor Rev. 16 (6), 593–609.
Strieter, R.M., Polverini, P.J., Kunkel, S.L., Arenberg, D.A., Burdick, M.D., Kasper, J., Dzuiba, J., Van Damme, J., Walz, A., Marriott, D., et al., 1995. The functional role of the ELR motif in CXC chemokine-mediated angiogenesis. J. Biol. Chem. 270 (45), 27348–27357.
Struyf, S., Burdick, M.D., Peeters, E., Van den Broeck, K., Dillen, C., Proost, P., Van Damme, J., Strieter, R.M., 2007. Platelet factor-4 variant chemokine CXCL4L1

inhibits melanoma and lung carcinoma growth and metastasis by preventing angiogenesis. Cancer Res. 67 (12), 5940–5948.
Struyf, S., Burdick, M.D., Proost, P., Van Damme, J., Strieter, R.M., 2004. Platelets release CXCL4L1, a nonallelic variant of the chemokine platelet factor-4/CXCL4 and potent inhibitor of angiogenesis. Circ. Res. 95 (9), 855–857.
Struyf, S., Salogni, L., Burdick, M.D., Vandercappellen, J., Gouwy, M., Noppen, S., Proost, P., Opdenakker, G., Parmentier, M., Gerard, C., Sozzani, S., Strieter, R.M., Van Damme, J., 2011. Angiostatic and chemotactic activities of the CXC chemokine CXCL4L1 (platelet factor-4 variant) are mediated by CXCR3. Blood 117 (2), 480–488.
Tattersall, P., Bratton, J., 1983. Reciprocal productive and restrictive virus-cell interactions of immunosuppressive and prototype strains of minute virus of mice. J. Virol. 46 (3), 944–955.
Taub, D.D., Lloyd, A.R., Conlon, K., Wang, J.M., Ortaldo, J.R., Harada, A., Matsushima, K., Kelvin, D.J., Oppenheim, J.J., 1993. Recombinant human interferon-inducible protein 10 is a chemoattractant for human monocytes and T lymphocytes and promotes T cell adhesion to endothelial cells. J. Exp. Med. 177 (6), 1809–1814.
Vandercappellen, J., Noppen, S., Verbeke, H., Put, W., Conings, R., Gouwy, M., Schutyser, E., Proost, P., Sciot, R., Geboes, K., Opdenakker, G., Van Damme, J., Struyf, S., 2007. Stimulation of angiostatic platelet factor-4 variant (CXCL4L1/PF-4var) versus inhibition of angiogenic granulocyte chemotactic protein-2 (CXCL6/GCP-2) in normal and tumoral mesenchymal cells. J. Leukoc. Biol. 82 (6), 1519–1530.
Vandercappellen, J., Van Damme, J., Struyf, S., 2011. The role of the CXC chemokines platelet factor-4 (CXCL4/PF-4) and its variant (CXCL4L1/PF-4var) in inflammation, angiogenesis and cancer. Cytokine Growth Factor Rev. 22 (1), 1–18.
Wetzel, K., Struyf, S., Van Damme, J., Kayser, T., Vecchi, A., Sozzani, S., Rommelaere, J., Cornelis, J.J., Dinsart, C., 2007. MCP-3 (CCL7) delivered by parvovirus MVMp reduces tumorigenicity of mouse melanoma cells through activation of T lymphocytes and NK cells. Int. J. Cancer 120 (6), 1364–1371.
Wrzesinski, C., Tesfay, L., Salome, N., Jauniaux, J.C., Rommelaere, J., Cornelis, J., Dinsart, C., 2003. Chimeric and pseudotyped parvoviruses minimize the contamination of recombinant stocks with replication-competent viruses and identify a DNA sequence that restricts parvovirus H-1 in mouse cells. J. Virol. 77 (6), 3851–3858.
Wu, Q., Dhir, R., Wells, A., 2012. Altered CXCR3 isoform expression regulates prostate cancer cell migration and invasion. Mol. Cancer 11, 3.
Zadori, Z., Szelei, J., Tijssen, P., 2005. SAT: a late NS protein of porcine parvovirus. J. Virol. 79 (20), 13129–13138.
Zipin-Roitman, A., Meshel, T., Sagi-Assif, O., Shalmon, B., Avivi, C., Pfeffer, R.M., Witz, I.P., Ben-Baruch, A., 2007. CXCL10 promotes invasion-related properties in human colorectal carcinoma cells. Cancer Res. 67 (7), 3396–3405.